Catalysis Science & Technology

Accepted Manuscript

ROYAL SOCIETY OF CHEMISTRY

www.rsc.org/catalysis

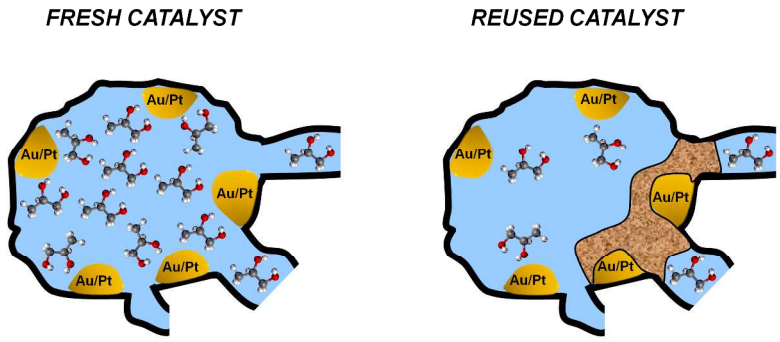

254x190mm (300 x 300 DPI)

Deactivation studies of a carbon supported AuPt nanoparticulate catalyst in the liquid-phase aerobic oxidation of 1,2-propanediol

Carmine D'Agostino[(a)], Yulia Ryabenkova[(b)], Peter J. Miedziak[(b)], Stuart H. Taylor[(b)], Graham J. Hutchings[(b)], Lynn F. Gladden[(a)] and Mick D. Mantle*[(a)]

[(a)] Department of Chemical Engineering & Biotechnology, University of Cambridge, Pembroke Street, Cambridge, CB2 3RA, UK.

[(b)] Cardiff Catalysis Institute, School of Chemistry, Cardiff University, Main Building, Park Place, Cardiff, CF10 3AT, UK.

*Corresponding Author:

Dr M.D. Mantle

Department of Chemical Engineering & Biotechnology

University of Cambridge

Pembroke Street

Cambridge

CB2 3RA, UK.

Email: mdm20@cam.ac.uk

Tel: + 44 (0) 1223-334777.

Abstract

The aerobic oxidation of 1,2-propanediol in alkaline aqueous solvent over bimetallic AuPt/C catalysts has been studied and catalyst reusability has been assessed. A systematic decrease of catalytic conversion was observed after each reuse of the catalyst. In order to understand the causes of deactivation, the catalyst samples were characterised by N_2 adsorption, temperature-programmed oxidation (TPO) and pulsed-field gradient nuclear magnetic resonance (PFG-NMR) diffusion measurements. The results revealed that the catalyst surface area and pore volume decrease significantly after each reuse of the catalyst. The intra-particle diffusion is characterised by two distinct diffusion regimes, a faster regime with self-diffusivities of 10^{-9} – 10^{-11} m^2 s^{-1} and a slow diffusion regime, with values of self-diffusivities on the order of 10^{-11} – 10^{-13} m^2 s^{-1}. Self-diffusivity in the fast regime is assigned to diffusion within the mesoporous space of the catalyst. Self-diffusivity in the slow diffusion region is assigned to diffusion within the microporous space and decreases after each reuse of the catalyst in a trend similar to that of pore volume, suggesting that changes in catalyst porosity and pore structure affect molecular mobility within the micropores. TPO studies of these systems showed a different distribution of oxidation products in the reused catalyst samples compared to the fresh catalyst, which suggests changes of the combustion mechanism. Altogether, the results reveal that catalyst deactivation is caused by deposition and build-up of heavy molecular species on the catalyst surface, which reduce the catalyst porosity by pore blockage and narrowing of channels, which in turn affects the diffusion rate within the micropores.

Keywords: Liquid-phase oxidation of 1,2-propanediol, gold catalysts, catalyst deactivation, PFG-NMR, diffusion

1. Introduction

Precious metal catalysts supported on activated carbon are widely used for the aerobic oxidation of alcohols [1] polyols like glycerol [2-4], propanediols [5-7] and sugars [8]. These alcohol oxidation reactions are of a great practical interest to a range of industries, as they lead to the formation of a wide range of commodities and fine chemicals.

It is well known that the life-time of a heterogeneous catalyst is often affected by several factors such as thermal and structural stability, sintering, fouling, site blocking, deposition of coke and other materials [9]. As a result, the catalytic activity decreases and this may lead to partial or even complete deactivation of the catalyst. The loss of activity in heterogeneous catalysts may be due to a number of different reasons, for example, the active sites of the catalyst within the pore space may be covered by coke or organic materials, hence preventing the adsorption of reactants. Moreover, the pores and channels of the catalyst may become partially or completely blocked due to changes in catalyst porosity, sintering of crystallites and/or deposition of external material. These changes in structural properties may also prevent the diffusing reactants from reaching the active sites with a consequent decrease of reaction rate.

The formation of "hard" coke, such as that formed during cracking reactions [10], in a liquid-phase oxidation reaction is highly unlikely, especially in the low temperature range (below 100 ºC) and in the presence of pure oxygen. However, Pintar *et al*. [11] reported that deposits of hydrocarbonaceous material, mostly in the condensed form of polyaromatics, can be formed during the liquid-phase oxidation of aqueous solutions of phenol over metal oxides at temperatures of approximately 700 ºC. The deposition of hydrocarbonaceous material as polyaromatic species and related catalyst deactivation have also been observed by Lakhapatri and Abraham [12,13] in several oxidation reactions occurring at high temperatures, including steam reforming of hydrocarbons [12] and jet fuel [13]. These are obviously very high

temperatures compared to those normally used in the oxidation of bio-derived feedstocks, such as glycols [5, 14, 15] and glycerol [1, 15], which are usually in the range 30–100 ºC. However, during reactions involving polyols, the production of unstable intermediates [5] may lead to the formation and build-up of high molecular weight species resulting from various types of side reactions such as condensation or polymerization of reactant and/or reaction intermediates and products [16]. Ide and Davis also reported that during the selective oxidation of diols, the adsorption of by-products, possibly as a result of such unwanted reactions, might be responsible for deactivating Pt supported catalyst [17].

Liquid-phase oxidation reactions of bio-derived feedstocks with molecular oxygen are often performed using supported gold catalysts. Density functional theory (DFT) studies of CO oxidation over supported gold catalysts have suggested that deactivation of gold nanoparticles may be due to the formation of stable carbonates on the catalyst surface [18]. Experimental evidence of carbonate-like species formation over Au supported catalyst surfaces has been provided by Hao *et al.* [19] using IR spectroscopy when studying CO oxidation over MgO-supported and CeO_2-supported gold catalysts. Accumulation of carbonate species continued throughout the reaction blocking the active sites on the catalyst surface. Raphulu *et al.* [20] reported similar findings using a Au/TiO_2 catalyst to oxidise CO.

Deactivation processes, either by deposition of coke or other carbonaceous materials, may lead to significant changes of the porous structure. Properties such as surface area, pore volume, pore size and tortuosity of the pore network may be significantly affected. Several techniques can be used to study deactivation processes, most notably nitrogen adsorption analysis [21], IR [22], XRD [23], TGA [22] and XPS [24]; these techniques have been important in identifying controlling factors, such as loss of surface area, adsorbed species, changes in crystal structure or mass loss of catalyst, and oxidation or reduction of surface species. PFG-NMR, which measures molecular self-diffusion, can also be used to probe the

causes of deactivation in a porous catalyst, since the technique is sensitive to any changes in catalyst pore structure *via* the influence of pore structure on molecular transport. For example, Wood *et al.* [21] used pulsed field gradient nuclear magnetic resonance PFG-NMR to study the effect of coke deposition on pore structure and diffusion in deactivated industrial hydroprocessing catalysts. The self-diffusivities of *n*-pentane and *n*-heptane probe molecules were found to decrease linearly with increasing coke content. It was also found that reductions of up to 16% in average BJH pore diameter, 40% in surface area of 48% in pore volume of the catalyst occurred in the most heavily coked samples compared with the fresh samples. PFG-NMR has also been used by Kortunov *et al.* [25] to study diffusion in FCC catalysts based on USY zeolite. The intra-particle self-diffusivity was found to decrease with increasing coke yield, suggesting changes in pore structure due to coke deposits.

In the current paper we focus on the use of a bimetallic AuPt/C catalysts for the aerobic liquid phase oxidation of 1,2-propanediol. We have recently reported that 1,2-propanediol can be successfully oxidised to lactic acid under mild conditions using AuPt/C supported heterogeneous catalyst prepared by sol immobilisation [7]. Au is known to act as an inhibitor to the deactivation of Pt or Pd catalysts [1]; however the AuPt/C catalyst we prepared still exhibits significant deactivation, thereby limiting its reusability. This prompted us to systematically investigate the deactivation process of this catalyst with several techniques including nitrogen adsorption, temperature programmed oxidation (TPO) and PFG-NMR diffusion measurements.

2. Experimental

2.1. Materials and chemical

1,2-propanediol (99%), sodium hydroxide (97%), *n*-octane (99%), polyvinylalcohol (80% hydrolyzed), $NaBH_4$ (96%) and activated carbon (Darco KB-B) were supplied by Sigma

Aldrich. $HAuCl_4$ and K_2PtCl_4 were supplied by Johnson Matthey. Deionised water was obtained from a laboratory purification system (PURELAB option, Elga).

2.2. Catalyst preparation

Aqueous solutions of $HAuCl_4$ (Johnson Matthey) and K_2PtCl_4 (Johnson Matthey) of the desired concentration were prepared. To this solution, polyvinylalcohol (PVA) (1 wt % solution, Sigma Aldrich, average molecular weight M_W = 9,000-10,000 g mol^{-1}, 80% hydrolysed) was added (PVA/metal (wt/wt) = 1.2). Subsequently, a freshly prepared 0.1 M solution of $NaBH_4$ (>96%, Aldrich, $NaBH_4$/Metal (mol/mol) = 5) was added to form a dark-brown sol. After 30 min of sol generation, the colloid was immobilised by adding activated carbon (Darco KB-B, Sigma Aldrich) and further acidified to pH 1 by sulfuric acid under vigorous stirring. The amount of support material required was calculated to give a total final metal loading of 1 wt%. After 1 h the slurry was filtered, the catalyst washed thoroughly with distilled water and dried at 110 ^oC overnight. Catalysts particles were in the range 50 – 150 micrometers.

2.3. Oxidation of 1,2-propanediol

Reactions were carried out using a 50 ml Radley's low pressure reactor. The 1,2-propanediol mixture (20 ml of 0.6M 1,2-propanediol in NaOH, diol/NaOH ratio = 1 or 2, mol/mol) and the catalyst ($1\%_{wt}$AuPt/C, 1,2-propanediol/metal ratio = 1000) were added into the reactor. The reactor was charged with oxygen (3 bar), heated to 40 ºC and maintained at temperature for 4 h under constant stirring (1000 rpm). The reaction mixture was cooled to room temperature and analyzed by NMR.

^{1}H NMR spectroscopy was used for product identification: spectra were acquired over a 16 scan period on a Bruker 400 MHz DPX system using a 5 mm auto tune broadband probe. All samples were prepared as dilute solutions in D_2O. All chemical shifts were acquired using TMS as the reference.

2.4. PFG-NMR experiments

PFG-NMR experiments were performed in a Bruker Biospin DMX 300 operating at a ^{1}H frequency of 300.13 MHz. The ^{1}H PFG-NMR experiments were carried out using a Bruker Biospin Diff-30 diffusion probe capable of producing magnetic field gradient pulses up to a strength of 11.76 T m^{-1}. Diffusion measurements of pure bulk liquids were performed using the PGSTE [26] pulse sequence, while APGSTE [27] sequences were used when studying diffusion of liquids within catalyst pellets to minimise the effects of background magnetic field gradients. The measurements were carried out holding the gradient pulse duration, δ, constant and varying the magnetic field gradient strength, g, in 16 increments. The observation time, Δ, was set 100 ms. The gradient pulse duration, δ, was set to 1 ms. 128 or 256 scans were acquired for each experiment, with a recycle time of 2 s and a gradient stabilisation delay of 1 ms.

To ensure consistency in sample preparation, a certain amount (~ 60 mg) of AuPt/C catalyst powder was placed in the NMR tube and loosely packed (i.e., without any compaction of the powder). The liquid of interest was then added such that supernatant liquid was present in the NMR tube. All NMR measurements were carried out at atmospheric pressure and 20 °C.

2.5. Nitrogen adsorption measurements

Nitrogen adsorption measurements on AuPt/C samples were carried out using a Micromeritics TriStar 3000 equipped with a V.6.08 A software for BET surface area and BJH

pore size analysis. Samples were degassed overnight. The sorption experiments were conducted taking sorption measurements in the relative pressure region of P/P_0 =0.01 to P/P_0 =0.995.

2.6. TPO measurements

TPO experiments were performed on a CATLAB-PCS (Hiden Analytical), comprising a microreactor module with integrated mass spectrometer. AuPt/C catalyst samples were loaded into the glass microreactor (11 mg for each experiment) and purged in a 40 ml min^{-1} flow of pure helium for 1 h. The flow was then switched from pure helium to 5% oxygen in helium and the temperature was ramped up to 900 ºC at a rate of 10 ºC min^{-1}. TPO profiles of CO, CO_2 and H_2O were recorded.

3. Results and discussion

3.1. Oxidation of 1,2-propanediol – Catalyst reusability tests

Extensive reusability studies using a 1 wt% AuPt/C catalyst were performed. Four subsequent reaction cycles (substrate:metal ratio 1000) were carried out to assess the reusability by varying the NaOH/substrate (NaOH:S) molar ratio from 1 to 2 equivalents. The catalytic data are presented in Table 1.

Table 1. Reusability tests for the oxidation of 1,2-propanediol with 1 wt% AuPt/C in aqueous NaOH[a].

Number of reaction cycles	NaOH/S[b]	Conversion [%]	Lactate [%]	Formate [%]	Acetate [%]	TOF [h^{-1}]
1	2	85	95	0	5	213
1	1	97	88	1	11	243
2	2	69	94	1	5	173
2	1	83	89	1	10	208
3	2	67	93	2	5	168
3	1	69	90	2	8	173
4	2	59	93	2	5	148
4	1	31	93	6	1	78

[a] Reaction conditions: water (20 ml), 1,2-propanediol (0.6 mol), oxygen 3 bar, 1,2-propanediol/total metal ratio = 1000, time = 4h, TOF calculated at 4h on the basis of total metal loading. Stirrer speed = 1000 rpm.
[b] NaOH:substrate molar ratio, where the substrate, S, is 1,2-propanediol.

Using a NaOH:S = 1 the reusability data showed a significant decrease in conversion after four cycles, decreasing from 97% to 31%. In contrast, by increasing the base concentration to two equivalents (NaOH:S = 2), the reusability was improved, showing a decrease of conversion from 85% to 59%. These data clearly indicate that deactivation is reduced at higher alkaline concentrations. This is consistent with the presence of base facilitating desorption of by-products, consequently minimising the poisoning effects of these species and therefore preserving catalytic activity, as reported in earlier work [28]. Increasing the amount of base from a ratio of 1 to 2 decreased conversion of the fresh catalyst slightly. Neither ratio may be the optimum for activity; however the influence of increasing the ratio on reducing catalyst deactivation is clear.

One common reason for catalyst deactivation may be the inhibition of catalytic sites by main reaction products. Therefore, the poisoning of catalyst by product inhibition, such as lactic acid, was checked by running the reaction in the presence of the product. However, the addition of the product to the initial reaction mixture did not cause any drop in conversion,

suggesting that poisoning caused by product inhibition does not occur. To investigate the reasons of the drop in conversion of 1,2-propanediol oxidation, a catalyst with the highest rate of deactivation (reused under a NaOH:S = 1) was chosen for further studies.

3.2. Nitrogen adsorption studies of fresh and reused catalyst

Adsorption isotherms for the fresh AuPt/C catalyst and after use in 4 cycles are reported in Figure 1. Type IV adsorption isotherms are observed in all cases [29]. Although the isotherms are similar in shape for both samples, the volume of gas adsorbed is significantly lower for the four times used sample (320 cm^3 g^{-1}) compared to the fresh catalyst (715 cm^3 g^{-1}). This suggests that a large decrease in catalyst porosity occurs after the catalyst has been used four times.

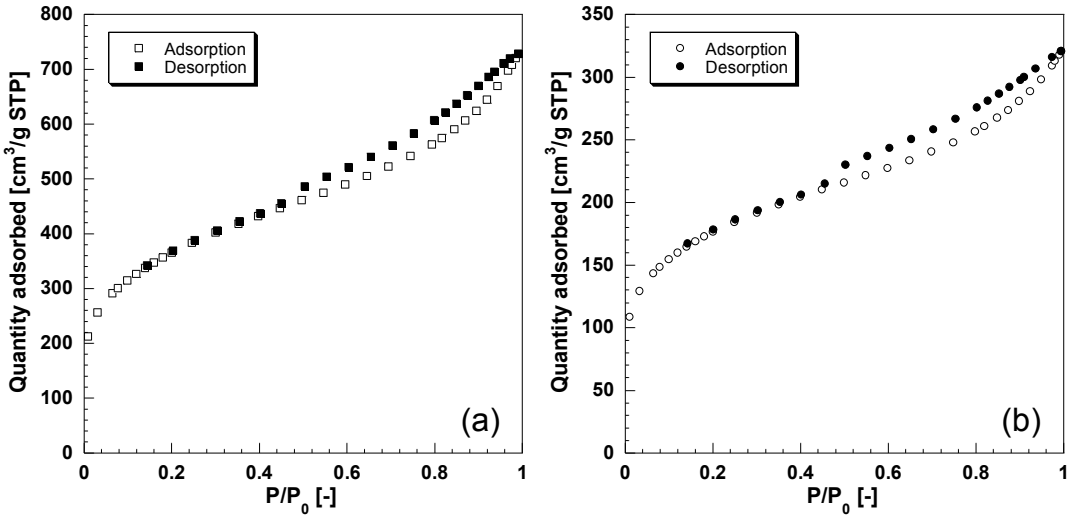

Figure 1. Nitrogen adsorption isotherms for: (a) AuPt/C fresh and (b) AuPt/C catalyst after 4 cycles of use. Note the amount of gas adsorbed for the used catalyst is much lower compared to the fresh sample.

The surface area from BET analysis, and pore volume and size from BJH analysis are reported in Table 2 for the AuPt/C samples.

Table 2. Results from nitrogen adsorption studies of fresh and reused AuPt/C samples.

Samples	Surface area [m^2 g^{-1}]	Pore volume [cm^3 g^{-1}]	Average pore size [nm]
AuPt/C fresh	1305	0.95	4.6
AuPt/C 1st run	910	0.56	4.5
AuPt/C 4th run	628	0.38	4.5

The results of nitrogen adsorption measurements clearly show that the pore volume of the catalyst is dramatically reduced after each cycle of use; for the 4th run catalyst the pore volume was more than 50% lower when compared to the fresh sample. A similar trend was observed for the surface area, which decreased from the initial value of 1305 m^2 g^{-1} to 628 m^2 g^{-1}. The average pore size remains essentially the same in all samples. The significant decrease of surface area and pore volume and the essentially unchanged average pore size of the samples suggest that the deposition of external materials within the catalyst matrix tends to build-up hindering or preventing the access of molecules to the pore space.

3.3. TPO analysis of fresh and reused catalysts

TPO profiles for fresh and reused AuPt/C catalyst samples are reported in Figure 2.

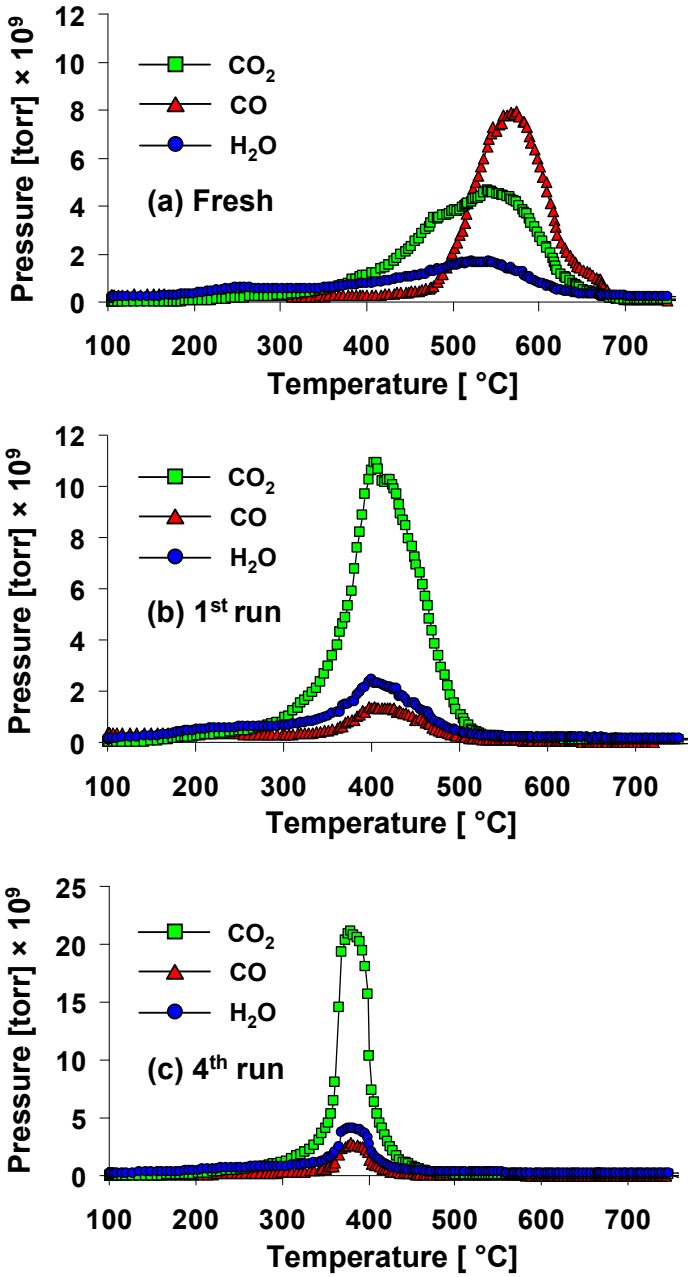

Figure 2. TPO profiles for CO_2, CO and H_2O in: (a) fresh, (b) 1st run and (c) 4th run AuPt/C samples. In the reused catalyst, the amount of H_2O and especially CO_2 is much higher compared to CO, as opposed to the fresh sample where CO is the main oxidation product.

A first major difference between the fresh AuPt/C and the reused samples is in the amount of CO_2 produced. For the fresh sample, CO is the main combustion product and its production is

higher than water and CO_2, as shown in Figure 3. Hueso *et al*. [30] reported a TPO profile for carbon particles similar to that observed from the fresh sample used in this work, with similar desorption temperatures and relative amounts of CO and CO_2. Here the reused catalysts show a significantly different product distribution. CO_2 is the main product and its production is much higher compared to CO. The production of H_2O is also higher than CO for both 1 and 4^{th} run catalysts compared to the fresh catalyst. A quantitative analysis showing the integral of the TPO profiles is shown in Figure 3 for the different species (CO, CO_2 and H_2O) in fresh and reused catalyst samples. Another major difference is in the value of the temperature of the observed peak maxima, especially when comparing the fresh with the two reused samples. For the fresh catalyst, the main oxidation peak occurs at approximately 570 ºC, with the peak of CO slightly shifted towards higher temperatures compared to CO_2 and H_2O. A broad shoulder is observed at lower temperatures for H_2O and is due to the water present on the catalyst surface, whereas H_2O observed at 570 ºC is water produced by combustion associated with the residues deposited onto the catalyst surface. Water from fresh activated carbon originates from the combustion of organic functional groups naturally present on the activated carbon surface [31]. For the once used catalyst, the combustion peaks are centred at approximately 400 ºC and for the catalyst used four times the combustion occurs at about 380 ºC.

The presence of abundant CO produced from the fresh sample, due to a partial oxidation of initial carbon, implies that carbon oxidation occurs in an atmosphere with low oxygen content. Conversely, the presence of CO_2 as the main product for the reused catalyst implies that oxidation occurs in a more oxygen rich environment, which favours the complete oxidation of the particles. The observation that all peaks in the TPO plot of reused catalysts are shifted to lower temperatures showing a unimodal distribution indicates that if external material is deposited on the activated carbon surface, it oxidises together with the carbon

support. Otherwise, two distinctive peaks would be observed, one for the activated carbon and the other for the organic species deposited on the surface. The presence of higher amounts of water produced in the reused catalyst samples is likely to derive from the oxidation of hydrocarbonaceous material accumulated within the catalyst pores after each reuse. The build-up of such material within the catalyst pores is likely to be due to side reactions, such as polymerisation and condensation, of reaction species. For example, hydroxyacetone, which is thought to be a key intermediate [5] for the production of lactates from 1,2-propanediol may be involved in the production of condensed products [5]. Hence, in the present work, it is plausible that formation of higher molecular weight complexes, which involves 1,2-propanediol and potentially one of its main intermediates, hydroxyacetone, may occur on the catalyst surface, which leads to build-up of residual material within the pores after the reaction.

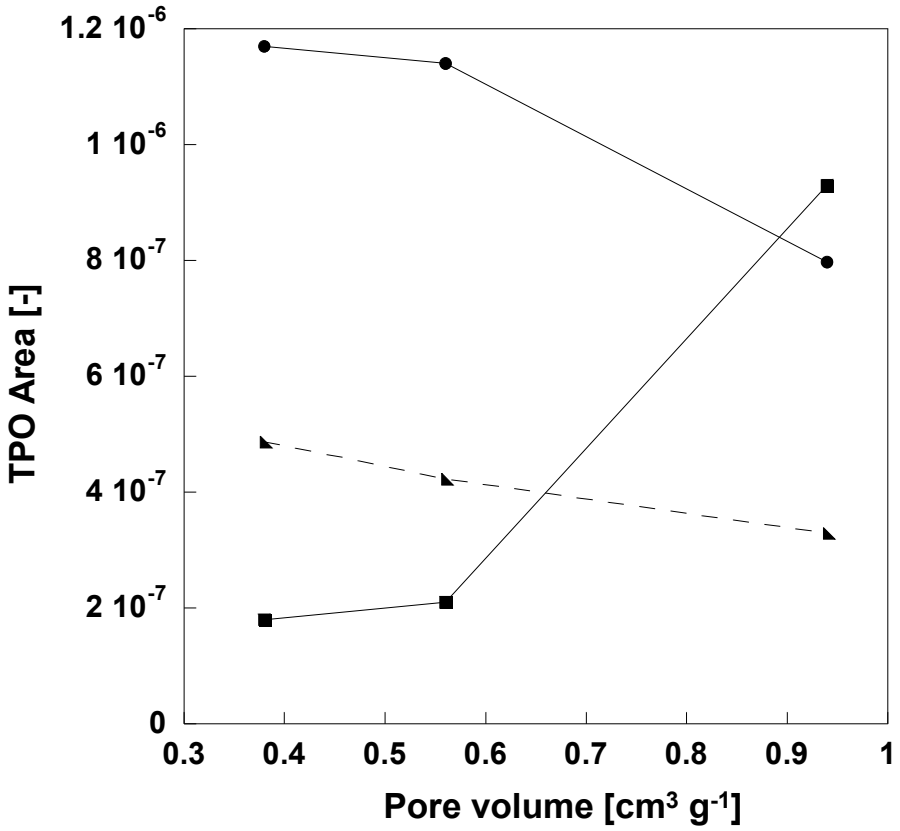

Figure 3. TPO area for CO_2 (●), CO (■) and H_2O (▼) as a function of pore volume. The pore volume decrease after each reuse of the catalysts. This corresponds to an increase in CO_2 and H_2O and indicates a change in the combustion regime and the presence of hydrocarbonaceous organic species deposited on the catalyst surface of the reused samples.

In general, the combustion of carbon particles usually proceeds between two limiting mechanisms: the homogeneous and the shell progressive [32]. The overall results of TPO analysis suggest that the reduction in porosity and internal surface area, due to deposition of high molecular weight species, affect the combustion process. A significant reduction in surface area and porosity, resulting in the blockage of micropores, could prevent oxygen from diffusing into the porous carbon support causing a shift from a "more" homogenous combustion mechanism towards a shell progressive mechanism. Therefore, oxidation would mostly take place on the outer surface of the catalyst particles, where a richer oxygen environment is present as compared to a homogeneous combustion of the carbon [33], favouring the complete oxidation of the carbon particles hence the production of CO_2 rather

than CO. A theoretical model for the combustion of porous carbon particles was developed by Gremyachkin [34]. It was reported that in diffusion-controlled oxidation the amount of CO_2 produced from the oxidative combustion of porous carbon, relative to CO, increases as the internal surface area decreases. This is consistent with the findings of the results presented here. According to Gremyachkin [34], as the internal surface area becomes smaller, the gas phase near the particle surface consists largely of CO_2. As the internal surface area becomes larger, the CO fraction in the gas phase near the particle surface increases, and for the largest possible surface area, the gas phase contains CO only. This theoretical prediction is indeed observed for the AuPt/C catalyst used in this work. The highest amount of CO is produced for the fresh sample, which also exhibits the highest surface area. As the surface area decreases, the amount of CO formed is reduced whilst CO_2 increased.

3.4. PFG-NMR diffusion studies of fresh and reused catalyst

3.4.1. PFG-NMR diffusion plots of fresh AuPt/C

In order to assess if and what changes occur in terms of molecular transport during the deactivation process, PFG-NMR self-diffusion measurements of various liquids of interest were carried out. The typical sample used for the PFG-NMR experiments contains liquid within and around the catalyst particles. In such conditions, a PFG-NMR experiment on such samples is expected to show at least two distinctive diffusion regimes, associated with the essentially unrestricted free liquid and the intra-particle space. Diffusion in the liquid between the catalyst particles will also be approximately that of the free liquid since the length scale probed by PFG-NMR experiments is of the order of a few micrometers [35], i.e., smaller than the length scale of the inter-particle space, which will be approximately that of the particles themselves (50 – 150 micrometers). In order to verify this, using the self-

diffusion coefficients of the bulk liquids subsequently presented, we have calculated the root mean square displacement $\left(RMSD = \sqrt{2Dt}\right)$, where D is the self-diffusion coefficient and t the observation time, equal to 100 ms in our case. The *RMSD* values were approximately 20 μm for *n*-octane and water, and 2 μm for 1,2-propanediol, values that are considerably smaller than the characteristic inter-particle space. Therefore, the liquid in the inter-particle space will mostly experience free unrestricted diffusion.

The PFG-NMR log attenuation plot of *n*-octane in the fresh AuPt/C catalyst is shown in Figure 4. Water and 1,2-propanediol also showed qualitatively similar plots (see supporting information Figure S1). As expected, the plots are non-linear. Experimental data were fitted with a three-component exponential decay in all cases (see Equation (1)). An attempt with a two-component model was made, but the use of two exponential terms did not provide a satisfactory agreement between the calculated and experimental curves (see supporting information Figure S2).

$$\frac{E(g)}{E_0} = p_{bulk}\exp\left[-bD_{bulk}\right] + p_{fast}\exp\left[-bD_{fast}\right] + p_{slow}\exp\left[-bD_{slow}\right] \qquad (1)$$

In Equation (1) b is the *b*-factor, $b = -\gamma^2 g^2 \delta^2 \left(\Delta - \delta/3\right)$, and p_i is the population of spins i with self-diffusivity value D_i, with i indicating bulk, fast or slow component.

The results suggest, therefore, the presence of three distinctive diffusion regions. The first region is expected to correspond to the unrestricted self-diffusivity of the *n*-octane molecules above and in between the catalyst particles. This was indeed confirmed by self-diffusion measurements performed on a tube filled only with liquid *n*-octane, which yielded a value of unrestricted self-diffusivity of 2.16×10^{-9} m^2 s^{-1}, in excellent agreement with D_{bulk} obtained from Equation (1), which gave a value of 2.20×10^{-9} m^2 s^{-1}, which is within the

experimental error. Obviously, D_{bulk} is the same for all samples as it is the unrestricted self-diffusivity of bulk *n*-octane. The other two regions are associated with the intra-particle space: a fast and slow component, D_{fast} and D_{slow}, respectively, can be observed. The fast component diffusivity of *n*-octane is approximately 50% slower compared to the bulk diffusivity and is essentially the same for fresh and reused samples, with a value of 1.22×10^{-9} m^2 s^{-1}. Similar decreases in self-diffusivity were also observed for water and 1,2-propanediol, with 1,2-propanediol showing self-diffusivities on the order of 10^{-11} m^2 s^{-1}. In order to ensure that this value of diffusivity represents intra-particle self-diffusion and *not* inter-particle self-diffusion, we have calculated the *RMSD* values associated with this diffusion component, analogous to that of the bulk liquid. The *RMSD* values for an observation time of 100 ms were approximately 15 μm for *n*-octane and water, and 1.5 μm for 1,2-propanediol. Therefore, during this observation time molecules do not move far enough on average to probe a representative portion of inter-particle space, which would be well above the characteristic particle size. Moreover, this value of diffusivity is significantly smaller (approximately 50% lower) than the unrestricted free liquid, which indicates that the liquid is confined within a tortuous pore space. This implies that this component has to be associated with molecules confined within the catalyst particles. Indeed, such drops of diffusivity with respect to the unrestricted bulk liquid self-diffusivity are typical of molecules confined in mesoporous structures [19, 36, 37].

Finally, the self-diffusivity in the intra-particle slow region is remarkably slow compared to both the bulk and fast intra-particle component. The values of the slow component of self-diffusivity for the different probe molecules are in the order of 10^{-11} (for octane and water) and 10^{-13} m^2 s^{-1} (for 1,2-propanediol), two orders of magnitude slower compared to bulk and fast components. Details of the values are reported in Table 3.

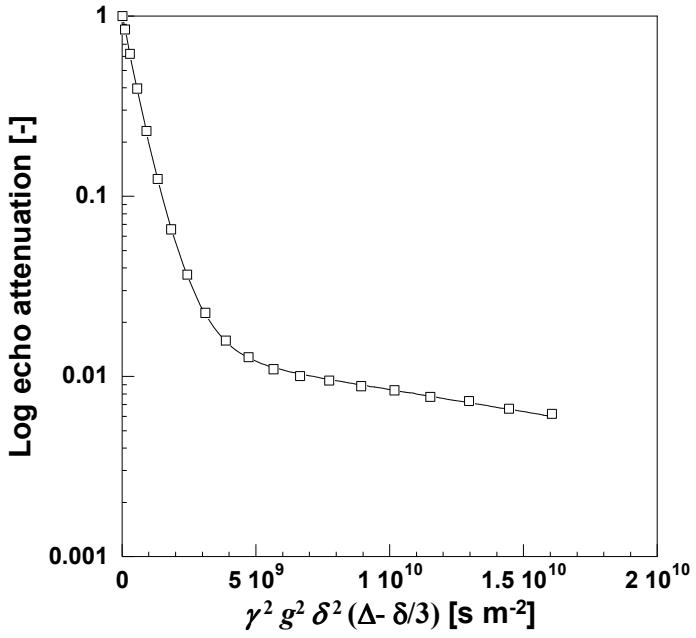

Figure 4. PFG-NMR log attenuation plot for *n*-octane in fresh AuPt/C. Solid lines are fitting to Equation (1).

Kortunov *et al.* [38] reported remarkably similar PFG-NMR diffusion plots when studying self-diffusion of 1,3,5-triisopropylbenzene (135-TPB) in USY and ammonium-ion exchanged zeolite Y used to produce the USY by zeolite steaming. They reported that of the total specific volume of mesopores (from 2 to 50 nm) and micropores (below 2 nm) of the USY zeolite, 40% of the volume is from mesopores and 60% from micropores. Kortunov *et al.*'s sample preparation for PFG-NMR experiments was performed in the same way as for this work. The choice of 135-TPB as one of the probe molecules for diffusion experiments was such that 135-TPB molecules are small enough to diffuse easily in the mesoporous region, but expected to have very small diffusivities in the micropores, or being unable in some cases to penetrate into the micropores at all. Three diffusion regions were observed, the first associated with the bulk free liquid around the particles, and the other two with the intra-particle space.

On the basis of all their PFG-NMR data, Kortunov *et al.* [38] concluded that intra-crystalline diffusion of guest molecules is essentially unaffected by mesopores in USY zeolite. This

interpretation of Kortunov can be understood by assuming that mesopores in USY crystals do not form a connected (i.e., percolation) network allowing diffusion of guest molecules through the crystals *via* only mesopores. The creation of such a diffusion pathway can be expected to lead to an order-of-magnitude increase in the characteristic intra-crystalline diffusivities in comparison to the mesopore-free crystals. This expectation is related to the possibility for guest molecules to diffuse out of zeolite crystals *via* only mesopores (i.e., very fast) as soon as they reach the mesopore volume for the first time. In contrast, if this diffusion pathway does not become available, only a moderate increase in the intracrystalline diffusivities can be expected due to generation of mesopores. Under such conditions, the diffusion process can be described as a consecutive diffusion through mesopores and micropores. The latter process is, obviously, the slowest one. Hence, the diffusion in the zeolite micropores is expected to limit the rate of the overall diffusion.

A knowledge of the pore structure is therefore very useful in order to better understand diffusion processes and hence catalytic data in porous materials. For the AuPt/C catalyst samples used in this work, nitrogen adsorption measurements were carried out to obtain information on the pore size distribution. The results revealed the presence of mesopores (up to 50 nm) but also a significant amount of micropores (below 2 nm). Croker *et al.* [39] reported that for the C support used in the AuPt/C catalyst preparation (activated carbon Darco KB-B) the pore size distribution shows approximately 7% of macropores, 70% of mesopores and 23% micropores. This pore size distribution is qualitatively similar to that of the samples used in the work of Kortunov *et al.* [38], which reported macropores represented by gaps between various crystal agglomerates of the zeolite bed within the NMR tube, besides the meso (~ 40% volume fraction of the intra-crystalline space) and micropores (~ 60% volume fraction of the intra-crystalline space) of the zeolite crystals. In this respect, the sample configuration is very similar to that described in this work. It has to be noted that a

quantitative comparison of the spin population, p_i, diffusing in each region cannot be made, because such a population will be affected by longitudinal (T_1) and transverse (T_2) relaxation during the diffusion time, which is highly dependent on the nature of the samples and may give values that do not represent the real spin distribution in each diffusion region.

Based on such observations, we associate the bulk diffusivity to the free liquid and possibly liquid within large macropores, the fast intra-particle diffusive component to the mesoporous region and the slow intra-particle diffusive component to the microporous region.

D_{bulk} ↔ Free liquid (possibly liquid in macropores)

D_{fast} ↔ Mesopores

D_{slow} ↔ Micropores

Indeed, the value of tortuosity [36, 37], that is, the ratio between the free self-diffusivity and the self-diffusivity within the pore space obtained by using a weak-interacting molecule (i.e., *n*-octane in our case), in the fast diffusive region is approximately 2, which is a typical value of alkanes diffusing in mesoporous materials [36, 37, 40, 41]. The PFG interaction parameter [37], that is, the ratio between the self-diffusivity of the free bulk liquid to that of the same liquid within the porous matrix, in the slow diffusive region has values as high as 100, which is usually not observed for mesoporous materials. In the microporous region, *n*-octane is expected to diffuse in the so-called configurational regime [42], that is, the size of the molecule is comparable to that of the pore/channel size. The mechanism of molecules diffusing in the configurational regime is, therefore, comparable to that of surface diffusion of adsorbed molecules on a surface [43]. Values of configurational diffusion can be significantly smaller compared to free diffusion [44], hence it is possible in the slow diffusive region, *n*-octane diffuses in such a regime. Large decreases in diffusivities, similar to these

observed in this work for the slow diffusive component, with respect to the unrestricted free self-diffusivity, have been reported for very similar molecules diffusing over the surface of catalyst pores [45], which is also a good indication of configurational diffusion, for the reasons previously highlighted. It has to be pointed out that the assignment of different diffusion regimes with different pore size regions implies the existence of macroscopic regions with different pore sizes (that is mesopores and micropores).

3.4.2. PFG-NMR diffusion in fresh and reused AuPt/C samples

The results of the PFG-NMR measurements for all guest molecules diffusing in fresh and reused samples are summarised in Table 3. The bulk self-diffusivity was reported only once as it is the same in all samples.

Table 3. Self-diffusivities obtained by fitting PFG-NMR experimental data to Equation (1).

Self-diffusivity $[m^2 s^{-1}] \times 10^{-11}$	Sample	*n*-Octane	Water	1,2-Propanediol
D_{bulk}	Bulk liquid	216 ± 7	205 ± 6	2.60 ± 0.08
D_{fast}	AuPt/C fresh	122 ± 4	143 ± 4	1.40 ± 0.04
	AuPt/C 1st run	127 ± 4	136 ± 4	1.35 ± 0.04
	AuPt/C 4th run	122 ± 4	131 ± 4	1.36 ± 0.04
D_{slow}	AuPt/C fresh	5.63 ± 0.16	4.03 ± 0.16	0.075 ± 0.002
	AuPt/C 1st run	3.40 ± 0.10	3.33 ± 0.10	0.063 ± 0.002
	AuPt/C 4th run	2.30 ± 0.10	3.00 ± 0.10	0.058 ± 0.002

Inspection of Table 3 for the self-diffusivity values within the pore space shows that D_{fast}, are approximately the same in all samples. Conversely the value of the slow component, D_{slow}, decreases after each time the catalyst is reused, particularly for *n*-octane. The results suggest that the reuse of catalyst is somehow affecting the structure of the microporous region.

Comparing PFG-NMR diffusion with nitrogen adsorption measurements, it can be observed that reduction of the self-diffusion coefficient in the slow diffusive region, as a function of the number of catalyst reuse cycles, is similar to the trend observed for the reduction of porosity. A plot of *n*-octane self-diffusivity for the D_{slow} component against catalyst pore volume for each sample is reported in Figure 5. The choice of alkanes as "more" suitable probe molecules for exploring changes in pore structure has been previously demonstrated [36, 37].

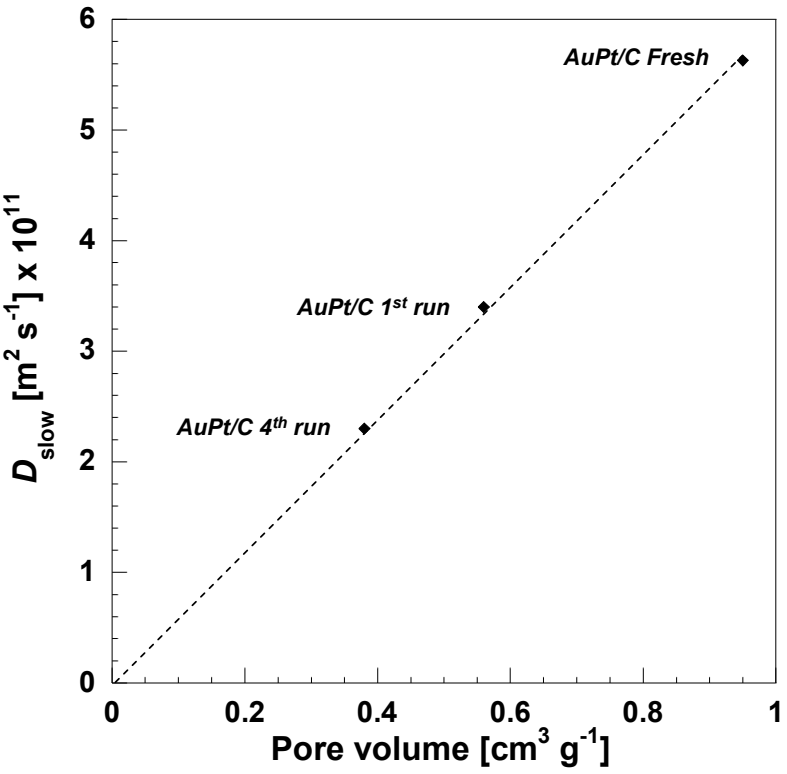

Figure 5. Plots of pore volume against self-diffusivity of *n*-octane in the slow diffusion region for fresh and reused AuPt/C samples. The dotted line is a linear fit to the experimental data.

Figure 5 shows a very clear linear trend between self-diffusivity in the slow region and pore volume, which implies that the decrease in catalyst porosity is significantly affecting self-diffusivity of guest molecules within the slow diffusion region, which is dominated by the

presence of micropores. This information, gathered by combining nitrogen adsorption analysis and PFG-NMR diffusion measurements, strongly suggests that the decrease in porosity is accompanied by narrowing of pore channels leading to pore blockage, which is particularly significant in the microporous region, hence retarding the diffusion of guest molecules.

Using the typical values of self-diffusion coefficients calculated for 1,2-propanediol, reported in Table 3, we have also carried out an analysis to estimate the presence of internal diffusion limitations, using the Weisz-Prater parameter [46]:

$$C_{WP} = \frac{-r\rho_c R^2}{D_i C_S} \qquad (2)$$

where $-r$ is the average reaction rate, calculated from the conversion data reported in Table 1, ρ_c the actual density of the catalyst (0.45 g cm^{-3}), R the typical catalyst particle radius, C_S the diol concentration and D_i the self-diffusion coefficient of the diol. According to the Weisz-Prater criterion, a value of $C_{WP} >> 1$ indicates the presence of severe diffusion limitations. Conversely, if $C_{WP} << 1$, there are no diffusion limitations. In order to calculate more accurate values of C_{WP}, one should have the self-diffusion coefficient of 1,2-propanediol highly diluted in water. Nonetheless, using the values of self-diffusivity reported in Table 3 it is still possible to have an estimate of C_{WP} values.

The Weisz-Prater parameter reported in Equation (2) was calculated once considering the self-diffusivity D_{fast}, associated to the mesopores, and once considering the self-diffusivity D_{slow}, associated with the micropores. Considering that the typical particle radii are in the range of 25 – 75 micrometers, for D_{fast} we have estimated typical values of $C_{WP} \approx 0.1-1$,

whereas for D_{slow} we have calculated values in the range of $C_{WP} \approx 2-20$. These values suggest that diffusion limitations exist within the micropores, which are also expected to affect catalytic activity and catalyst reusability.

4. Conclusions

Catalyst reusability tests have been carried for the aerobic oxidation of 1,2-propanediol in alkaline aqueous solvent over AuPt/C catalyst. Reaction studies showed a systematic decrease of catalyst activity after each reaction run. In order to elucidate the catalyst deactivation process, nitrogen adsorption and TPO analysis were used in conjunction with PFG-NMR diffusion measurements. The combined results of the different techniques used show that it is possible to obtain a picture of the catalyst deactivation process, which involves the formation and build-up of deposits of high molecular weight carbonaceous species within the pore space, as a result of side-reactions such as condensations or polymerizations. These deposits contribute to a significant blockage of pores, particularly in the microporous region, where the self-diffusion coefficient of guest molecules decreases linearly with the catalyst pore volume. Additional analysis also revealed the presence of diffusion limitations in the microporous region of the catalyst, which will further affect catalyst activity and reusability. The results presented in this work demonstrate the usefulness of the PFG-NMR technique to study deactivation processes in heterogeneous catalysis. Combining this technique with more conventional methods it is possible to gain new insights into deactivation of heterogeneous catalysts and hence adopt suitable strategies in order to minimise the rate of deactivation by choosing, for example, a material with an optimal pore size distribution and pore connectivity.

Acknowledgments

The authors would like to acknowledge the Technology Strategy Board for funding this work, Grant No. TP/7/ZEE/6/I/N0262B. The Technology Strategy Board is a government body, which promotes and supports the development and exploitation of technology and innovation for the benefit of UK business, in order to increase economic prosperity and improve quality of life. For more information see www.innovateuk.org. We also wish to thank EPSRC for funding the CASTech consortium (EP/G011397/1) and Platform Grant (EP/F047991/1), both of which supported this work.

References.

[1] Enache, D. I., Edwards, J. K., Landon, P., Solsona-Espriu, B., Carley, A. F., Herzing, A. A., Watanabe, M., Kiely, C. J., Knight, D. W. and Hutchings, G. J., "Solvent-free oxidation of primary alcohols to aldehydes using Au-Pd/TiO2 catalysts", *Science* **311**, 362-365, (2006).

[2] Bianchi, C. L., Canton, P., Dimitratos, N., Porta, F. and Prati, L., "Selective oxidation of glycerol with oxygen using mono and bimetallic catalysts based on Au, Pd and Pt metals", *Catalysis Today* **102**, 203-212, (2005).

[3] Demirel, S., Lehnert, K., Lucas, M. and Claus, P., "Use of renewables for the production of chemicals: Glycerol oxidation over carbon supported gold catalysts", *Applied Catalysis B: Environmental* **70**, 637-643, (2007).

[4] Demirel-Gulen, S., Lucas, M. and Claus, P., "Liquid phase oxidation of glycerol over carbon supported gold catalysts", *Catalysis Today* **102**, 166-172, (2005).

[5] Prati, L. and Porta, F., "Oxidation of alcohols and sugars using Au/C catalysts - Part 1. Alcohols", *Applied Catalysis A: General* **291**, 199-203, (2005).

[6] Prati, L. and Rossi, M., "Gold on carbon as a new catalyst for selective liquid phase oxidation of diols", *Journal of Catalysis* **176**, 552-560, (1998).

[7] Ryabenkova, Y., He, Q., Miedziak, P.J., Dummer, N.F., Taylor, S.H., Carley, A. F., Morgan, D. J., Dimitratos, N., Willock, D.J., Bethell, D., Knight, D.W., Chadwick, D., Kiely, C. J. and Hutchings, G.J. "The selective oxidation of 1,2-propanediol to lactic acid using mild conditions and gold-based nanoparticulate catalysts", *Catalysis Today,* **203**, 139-145, (2013).

[8] Comotti, M., Della Pina, C., Matarrese, R., Rossi, M. and Siani, A., "Oxidation of alcohols and sugars using Au/C catalysts - Part 2. Sugars", *Applied Catalysis A: General* **291**, 204-209, (2005).

[9] Mallat, T. and Baiker, A., "Oxidation of alcohols with molecular oxygen on solid catalysts", *Chemical Reviews* **104**, 3037-3058, (2004).

[10] Le Minh, C., Chaoen, L. and Brown, T. C., "Kinetics of coke combustion during temperature-programmed oxidation of deactivated cracking catalysts", Catalyst Deactivation 1997; Bartholomew, C. H., Fuentes, G. A., Eds.; Amsterdam: Elsevier Science, **111**, 383-390 (1997).

[11] Pintar, A., Bercic, G. and Levec, J., "Catalytic liquid phase oxidation of aqueous phenol solutions in a trickle-bed reactor", *Chemical Engineering Science* **52**, 4143-4153, (1997).

[12] Lakhapatria, S. L., Abraham, M. A., "Deactivation due to sulfur poisoning and carbon deposition on Rh-Ni/Al_2O_3 catalyst during steam reforming of sulfur-doped n-hexadecane", *Applied Catalysis A: General* **364**, 113–121 (2009).

[13] Lakhapatria, S. L., Abraham, M. A., "Analysis of catalyst deactivation during steam reforming of jet fuel on Ni-(PdRh)/γ-Al_2O_3 catalyst", *Applied Catalysis A: General* **405**, 149-159 (2011).

[14] Bianchi, C., Porta, F., Prati, L. and Rossi, M., "Selective liquid phase oxidation using gold catalysts", *Topics in Catalysis* **13**, 231-236, (2000).

[15] Dimitratos, N., Lopez-Sanchez, J. A., Meenakshisundaram, S., Anthonykutty, J. M., Brett, G., Carley, A. F., Taylor, S. H., Knight, D. W. and Hutchings, G. J., "Selective formation of lactate by oxidation of 1,2-propanediol using gold palladium alloy supported nanocrystals", *Green Chemistry* **11**, 1209-1216, (2009).

[16] Suprun, W., Lutecki, M., Haber, T. and Papp, H., "Acidic catalysts for the dehydration of glycerol: Activity and deactivation", *Journal of Molecular Catalysis A: Chemical* **309**, 71–78 (2009).

[17] Ide, M. and Davis, R. J., "Selective oxidation of diols over supported Pt catalysts in base-free aqueous solution", *12 AIChE annual meeting*, Pittsburg, PA.

[18] Qian, K., Zhang, W., Sun, H., Fang, J., He, B., Ma, Y., Jiang, Z., Wei, S., Yang, J. and Huang, W., "Hydroxyls-induced oxygen activation on "inert" Au nanoparticles for low-temperature CO oxidation", *Journal of Catalysis* **277**, 95-103, (2011).

[19] Hao, Y., Mihaylov, M., Ivanova, E., Hadjiivanov, K., Knözinger, H. and Gates, B. C., "CO oxidation catalyzed by gold supported on MgO: Spectroscopic identification of carbonate-like species bonded to gold during catalyst deactivation", *Journal of Catalysis* **261**, 137-149, (2009).

[20] Raphulu, M. C., McPherson, J. S., van der Lingen, E., Anderson, J. A. and Scurrell, M. S., "Investigation of the active site and the mode of Au/TiO_2 catalyst deactivation using Diffuse Reflectance Infrared Fourier Transform Spectroscopy (DRIFTS)", *Gold Bulletin* **43**, 21-28, (2010).

[21] Wood, J. and Gladden, L. F., "Effect of coke deposition upon pore structure and self-diffusion in deactivated industrial hydroprocessing catalysts", *Applied Catalysis A: General* **249**, 241-253, (2003).

[22] Li, B., Gonzalez, R.D., "TGA/FT-IR studies of the deactivation of sulfated zirconia catalysts", *Applied Catalysis A: General* **165**, 291-300, (1997)

[23] Fang, J., Li, Z., Xu, G., Wang, B, Xiang, T., Effect of Temperature on the Deactivation of a Pd-Fe/α-Al_2O_3 catalyst for CO coupling to diethyl oxalate, *Journal of Natural Gas Chemistry* **12**, 243-246, (2003).

[24] Vass, E.M., Teschner, D., Hävecker, M., Zafeiratos, S., Schnörch, P., Knop-Gericke, A., Schlögl, R., Dehydrogenation and oxidative dehydrogenation of n-butane using vanadium based catalysts: an in situ XPS study, Bessy Annual Reports 94-96, (2006).

[25] Kortunov, P., Vasenkov, S., Kärger, J., Fe Elıa, M., Perez, M., Stocker, M., Papadopoulos, G. K., Theodorou, D., Drescher, B., McElhiney, G., Bernauer, B., Krystl, V., Kocirik, M., Zikanova, A., Jirglova, H., Berger, C., Glaser, R., Weitkamp, J. and Hansen, E.

W., "Diffusion in fluid catalytic cracking catalysts on various displacement scales and its role in catalytic performance", *Chem. Mater.* **17**, 2466-2474, (2005).

[26] Stejskal, E. O. and Tanner, J. E., "Spin diffusion measurements: spin echoes in the presence of a time-dependent field gradient", *Journal of Chemical Physics* **42**, 288-292, (1965).

[27] Cotts, R. M., Hoch, M. J. R., Sun, T. and Markert, J. T., "Pulsed field gradient stimulated echo methods for improved NMR diffusion measurements in heterogeneous systems", *Journal of Magnetic Resonance* **83**, 252-266, (1989).

[28] Dimitratos, N., Villa, A., Wang, D., Porta, F., Su, D. S. and Prati, L., "Pd and Pt catalysts modified by alloying with Au in the selective oxidation of alcohols", *Journal of Catalysis* **244**, 113-121, (2006).

[29] Balbuena, P. B. and Gubbins, K. E., "Classification of adsorption behaviour - simple fluids in pores of slit-shaped geometry", *Fluid Phase Equilibria* **76**, 21-35, (1992).

[30] Hueso, J.L., Caballero, A., Ocañaa, M. and González-Elipe, A. R., "Reactivity of lanthanum substituted cobaltites toward carbon particles", *Journal of Catalysis* **257** 334-344, (2008).

[31] Valdes, H., Sanchez-Polo, M., Rivera-Utrilla, J. and Zaror, C. A., "Effect of ozone treatment on surface properties of activated carbon", *Langmuir* **18**, 2111-2116, (2002).

[32] Doraiswamy, L. K. and Sharma, M. M., Heterogeneous Reactions, Vol. 1. Wiley & Sons, New York, USA (1984).

[33] Zajdlik, R., Markos, J., Jelemensky, L. and Remiarova, B., "Single coal char particle combustion in the carbon dioxide atmosphere", *Chem. Papers* **54**, 467-472 (2000).

[34] Gremyachkin, V. M., "Combustion of porous carbon particles in oxygen", *Theoretical Foundations of Chemical Engineering* **34**, 381-390, (2000).

[35] Hollewand, M. P. and Gladden, L. F., "Transport heterogeneity in porous pellets. 1. PGSE NMR studies", *Chemical Engineering Science* **50**, 309-326, (1995).

[36] Mantle, M. D., Enache, D. I., Nowicka, E., Davies, S. P., Edwards, J. K., D'Agostino, C., Mascarenhas, D. P., Durham, L., Sankar, M., Knight, D. W., Gladden, L. F., Taylor, S. H. and Hutchings, G. J., "Pulsed-field gradient NMR spectroscopic studies of alcohols in supported gold catalysts ", *Journal of Physical Chemistry C* **115**, 1073-1079, (2011).

[37] D'Agostino, C., Mitchell, J., Gladden, L. F. and Mantle, M. D., "Hydrogen bonding network disruption in mesoporous catalyst supports probed by PFG-NMR diffusometry and NMR relaxometry", *Journal of Physical Chemistry C*, **116**, 8975-8982, (2012).

[38] Kortunov, P., Vasenkov, S., Karger, J., Valiullin, R., Gottschalk, P., Elia, M. F., Perez, M., Stocker, M., Drescher, B., McElhiney, G., Berger, C., Glaser, R. and Weitkamp, J., "The role of mesopores in intracrystalline transport in USY zeolite: PFG NMR diffusion study on various length scales", *Journal of the American Chemical Society* **127**, 13055-13059, (2005).

[39] Crocker, M., Graham, U. M., Gonzalez, R., Jacobs, G., Morris, E., Rubel, A. M. and Andrews, R., "Preparation and characterization of cerium oxide templated from activated carbon", *Journal of Materials Science* **42**, 3454-3464, (2007).

[40] D'Agostino, C., Brett, G. L., Miedziak, P. J., Knight, D. W., Hutchings, G. J., Gladden, L. F. and Mick D. Mantle, "Understanding the solvent effect on the catalytic oxidation of 1,4-butanediol in methanol over Au/TiO_2 catalyst: NMR diffusion and relaxation studies", *Chem. Eur. J.* **18**, 14426-14433 (2012).

[41] D'Agostino, C., Kotionova, T., Mitchell, J., Miedziak, P. J., Knight, D. W., Taylor, S.H., Hutchings, G. J., Gladden, L. F. and Mick D. Mantle, "Solvent effect and reactivity trend in the aerobic oxidation of 1,3-propanediols over gold supported on Titania: NMR diffusion and relaxation studies", *Chem. Eur. J.* **19**, 11725 – 11732 (2013).

[42] Chen, N. Y., Degnan, T. F., Smith, C. M., “Molecular Transport and Reaction in Zeolites: Design and Application of Shape Selective Catalysts”, Wiley-VCH, Weinheim, Germany (1994).

[43] Stallmach, F. and Karger, J., “The potentials of pulsed field gradient NMR for investigation of porous media”, *Adsorption* **5**, 117–133 (1999).

[44] Nakasaka, Y., Tago, T., Yano, K. and Masuda, T., "Liquid-phase diffusivity of benzene within mesoporous materials measured by a laser Raman technique", *Chemical Engineering Science* **65**, 226-231, (2010).

[45] Weber, D., Sederman, A. J., Mantle, M. D., Mitchell, J. and Gladden, L. F., “Surface diffusion in porous catalysts”, *Physical Chemistry Chemical Physics*, **12**, 2619-2624, (2010).

[46] Fogler, H. S., Elements of Chemical Reaction Engineering, Prentice Hall, New Jersey, USA (2005).